EURASIAN JOURNAL OF MATHEMATICAL AND COMPUTER APPLICATIONS
ISSN 2306–6172
Volume 13, Issue 2 (2025) 75 – 82

NUMERICAL SIMULATION OF THE DYNAMICS OF DISPERSE PHASE PARTICLES IN A SUPERSONIC FLOW BEHIND THE SHOCK WAVE

Polyansky T.A., Zaitsev A.V. [1]

Abstract The paper describes the results of the development of a numerical technique for calculating supersonic two-phase flows. The program implementation of this technique is presented. Verification of the interphase interaction models is performed on the basis of experimental data on interaction of a supersonic flow with a cloud of particles in a shock tunnel for various particle concentrations.

Key words: Shock wave, Two phase flow, CFD, OpenFOAM.

AMS Mathematics Subject Classification: 76L05, 76T15.

DOI: 10.32523/2306-6172-2025-13-2-75-82

1 Introduction

Supersonic two-phase flows are encountered in various areas, including industry and aerospace engineering. Investigations of physical phenomena arising in such flows is of great significance for practice. The primary phenomenon of interest is the influence of the disperse phase on the carrier gas flow. One of the examples of such flows is gas exhaustion into a rarefied space, where large clusters of the condense gas are formed under certain conditions. Such processes are mainly studied in experiments with the use of large [1] or small (laboratory-scale) [2] vacuum gas-dynamic facilities. However, this approach requires large material and financial expenses because a high degree of rarefaction in the test section has to be maintained. In addition, it is rather difficult to reproduce the full spectrum of natural conditions. Some problems of using experimental methods can be avoided by using numerical simulations. A detailed study of the problem of gas jet exhaustion into a rarefied space reveals the existence of two characteristic zones. The first one is the external flow in the rarefied space. In this zone, the gas flow proceeds in the free-molecular regime. Such flows are modeled by approaches based on solving kinetic equations, e.g., by the Direct Simulation Monte Carlo (DSMC) method [3]. The second zone corresponds to the continuum flow regime in the nozzle and in the near field in an immediate vicinity of the nozzle. In this zone, the gas density is sufficiently high, which makes the use of DSMC methods computationally expensive. Therefore, an effective method to be used in this zone is the multizonal approach [4], where the flow in the nozzle is calculated by equations of continuous media, while the jet in the free space is calculated by the DSMC method. For each zone, it is necessary to develop appropriate numerical tools for modeling the disperse phase. In the present study, our attention is focused on the second zone. The final goal of investigations is to consider the dynamics of particle motion and the influence of particles on the process of gas exhaustion from the nozzle. At the present stage, we choose the model, its implementation and verification on the basis of experimental data. In the continuum zone, there are several approaches to modeling two-phase flows. In the so-called Eulerian-Eulerian approach, the second zone is presented as a separate gas consisting of particles, which allows one to use a

[1] Corresponding Author.

similar set of equations. The basic principles and mechanisms of interphase interaction based on this approach were described, e.g., by Nigmatulin [5]. Interphase influence if organized via the corresponding source terms in equations for the gas and disperse medium. The method has certain advantages, but there are also significant constraints. Using this method, one can obtain only averaged characteristics of the disperse phase, which can appreciably distort the real pattern, e.g., in the case of particle reflection from the walls. In our study, we chose the Euler-Lagrangian approach [6]. In this method, the gas dynamics is described by a system of continuum equations, while the disperse phase is presented by a set of discrete particles, each being described by its own equation of motion under the action of gas-dynamic forces. Similar to the first case, the mechanism of the reverse influence of particles on the gas is realized via additional source terms in the equations, but their calculation is a separate problem. This method was already applied for modeling supersonic two-phase flows. Bular et al. [7] used this approach for modeling shock wave interaction with a cloud of particles with due allowance for the reverse influence of particles. Similar investigations were performed by Sugiyama et al. [8]. Peng et al. [9] considered the scatter of disperse particles under the action of a shock wave. One of the key issues is determination of the interphase interaction coefficients because theoretical models are always not applicable. In this situation, one has to use various semi-empirical models, and it is necessary to verify whether these models can be applied under particular conditions.

2 Mathematical model

In the chosen approach, the gas-dynamic flow pattern is obtained by solving the Navier-Stokes equations. We consider a single-species medium without chemical reactions. In this case, the system consists of the continuity equation, momentum conservation law, and energy conservation law. The initial equations are modified by inserting additional source terms, which model the reverse influence of the disperse phase on the carrier gas:

$$\frac{\partial \rho}{\partial t} + \nabla \cdot (\rho \vec{u}) = 0, \qquad \frac{\partial \rho \vec{u}}{\partial t} + \nabla \cdot (\rho \vec{u} \cdot \vec{u}) = -\nabla P + \nabla \cdot \hat{\tau} + S_p,$$

$$\frac{\partial \rho E}{\partial t} + \nabla \cdot (\rho E \cdot \vec{u}) = \nabla \cdot (\lambda \nabla T) + \nabla \cdot (\hat{\tau} \cdot \vec{u}) + S_q$$

$$\hat{\tau} = \left(-\frac{2}{3}\mu \nabla \cdot \vec{u}\right)\delta_{ij} + \mu\left(\nabla \vec{u} + (\nabla \vec{u})^T\right); \qquad E = e + \frac{1}{2}|\vec{u}^2|.$$

The system is closed by the equation of state for an ideal gas $p = \rho RT/\mu_{mol}$. In the Lagrangian formulation, each particle of the disperse phase is described by an individual equation:

$$\frac{d(m_p \vec{u_p})}{dt} = \sum \vec{F_i}.$$

The motion occurs under the action of external forces. The main contribution is made by the aerodynamic drag force

$$\vec{F_d} = \frac{1}{2} C_d \pi r_p^2 \rho_g (\vec{u_g} - \vec{u_p})|\vec{u_g} - \vec{u_p}|.$$

A key issue here is determination of the drag coefficient C_d. For subsonic flows, a simple dependence on the Reynolds number is widely used. In the present study, we consider three models.

Model 1 is the classical expression of the drag coefficient as a function of the Reynolds number The Reynolds number is calculated on the basis of the particle diameter and local relative velocity as $\mathrm{Re} = 2r_p|\vec{u_g} - \vec{u_p}|/\mu_g$. A transition to supersonic regimes requires the effects arising thereby to be taken into account and additional corrections to be used. As the processes are very complicated, it does not seem possible to derive an analytical expression; therefore, various semi-empirical correlations are used in practice.

Model 2 is the model developed by Boiko et al. [10], which is a simple dependence on the Reynolds number and relative Mach number:

$$C_d = \frac{24}{\mathrm{Re}}\left(1 + \frac{1}{6}\mathrm{Re}^{\frac{2}{3}}\right).$$

There are more complicated models, which take into account the rarefaction effects.

Model 3 is a more complicated correlation proposed by Henderson [11]. The dependence in the subsonic region has the form

$$\begin{aligned} C_d &= 24\left[\mathrm{Re} + s\left(4.33 + \left(\frac{3.65 - 1.53T_p/T_g}{1 + 0.353T_p/T_g}\right)e^{-0.247\mathrm{Re}/s}\right)\right]^{-1} \\ &+ e^{-0.5\mathrm{M}/\sqrt{\mathrm{Re}}}\left[\frac{4.5 + 0.38(0.03\mathrm{Re} + 0.48\sqrt{\mathrm{Re}})}{1 + 0.03\mathrm{Re} + 0.48\sqrt{\mathrm{Re}}} + 0.1\mathrm{M}^2 + 0.2\mathrm{M}^8\right] + 0.6\left[1 - e^{-\mathrm{M}/\mathrm{Re}}\right]s. \end{aligned}$$

A different function is used for supersonic flows beginning from the Mach number of 1.75. Linear interpolation of the values of both functions at the ends of the interval is applied between the zones:

$$C_d = \left(0.9 + \frac{0.34}{\mathrm{M}^2} + 1.86\sqrt{\frac{\mathrm{M}}{\mathrm{Re}}}\left[2 + \frac{2}{s^2} + \frac{1.059}{s}\sqrt{\frac{T_p}{T_g}} - \frac{1}{s^4}\right]\right) \Big/ \left(1 + 1.86\sqrt{\frac{\mathrm{M}}{\mathrm{Re}}}\right).$$

In addition to the already mentioned Reynolds number, this formula includes the Mach number also based on the difference between the particle and carrier gas velocities, gas temperature T_g and particle temperature T_p, while the molecular speed ratio is calculated as $s = \mathrm{M}\sqrt{\gamma/2}$. Brief overview of models are listed in Tab. 1.

Practical implementation of the gas-dynamic solver and drag coefficient models is performed on the basis of the OpenFOAM open-source library for finite volume computations [12]. The basis is the rhoCentralFoam source code of the solver, and the algorithm is supplemented with library components responsible for modeling a cloud of the Lagrangian particles. For implementation of the above-presented models of interphase interaction, we also wrote a user library containing both the models proper and the extended version of the thermoCloud standard structure necessary for operation of these models. Integration with respect to time is performed by the first-order Eulerian scheme. Spatial discretization is based on the Kurganov-Tadmor numerical scheme within the second order of accuracy. The reverse influence mechanism is implemented via the source terms. For the momentum equation, it is the sum of force interaction over all particles in the control volume V:

$$\vec{S_p} = -\sum_{i=1}^{N}\frac{\vec{F_{di}}}{V}.$$

3 Choosing the verification problem

Verification of the numerical tools described above requires comparisons with experimental results. In this case, it is convenient to consider the problem of interaction of a supersonic in a shock tunnel with a cloud of particles. In such a formulation, one can obtain both qualitative and quantitative results for various values of parameters. In the present study, we consider

Table 1: List of models

Models	Model 1, Classical	Model 2, [10]	Model 3, [11]
Parameters	Re	Re, M	Re, M, T_g, T_p, γ

the experiments of Boiko et al. [10]. The arrangement of the experiments is illustrated in Fig. 1.

The experimental setup is a channel with a square cross section 52 mm wide separated by a membrane into two zones. The first one is the test section with a transparent window in the wall for optical diagnostic tools, pressure sensors, and the mechanism for particle cloud formation. The second zone is the high-pressure chamber where a supersonic flow is formed after membrane breakdown. The gas parameters in both zones are listed in Tab. 2. They ensure the formation of a supersonic flow with the Mach number of 2.8. Two types of particles (plastic and bronze) were used in the experiments to form a cloud of particles. The particle properties are listed in Tab. 3. In all cases, the particles are assumed to be spherical and to have the same size.

4 Formulation of the numerical problem

In accordance with the experimental conditions, we performed numerical simulations of the flow in some part of the channel. A three-dimensional grid consisting of 2.8 million cubic cells was generated in a rectangular computational domain 52x52x125 mm. The channel walls were subjected to the no-slip condition. The zero-gradient conditions for pressure, temperature, and velocity were imposed at the open end-face boundaries. The distributions of the gas parameters in the volume at the initial time were set according to the zones shown in Fig. 2. A cloud of particles with a specified volume fraction was placed at the interface between the zones ahead of the shock wave.

5 Results of numerical simulations

Qualitative comparisons were performed at the first stage. For a small volume fraction of particles, we calculated the patterns of supersonic flow interaction with individual particles.

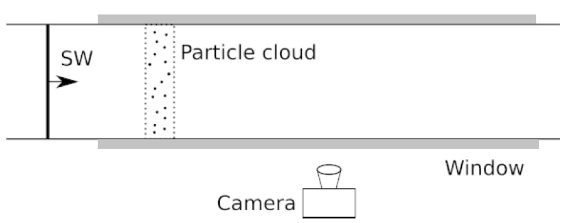

Figure 1: Arrangement of the experiments.

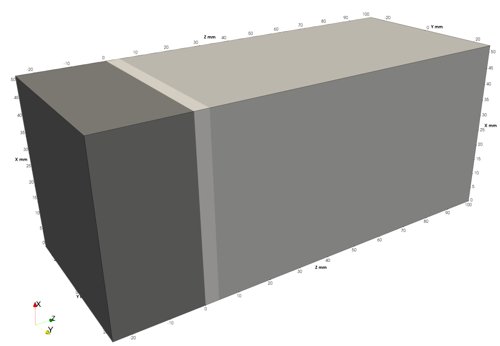

Figure 2: Computational domain. The dark region is the high-pressure zone, and the adjacent light region is the zone where the particle cloud is located.

Table 2: Gas parameters

	High-pressure zone	Test section
Pressure, MPa	0.89	0.1
Temperature, K	735	300
Density, kg/m^3	4.426	1.158
Velocity, m/s	705	0

Table 3: Particle parameters in the experiments

Particle diameter, νm	Density, kg/m^3	Volume fraction, %
130	8600	0.1
130	8600	1
300	1200	0.1
300	1200	3

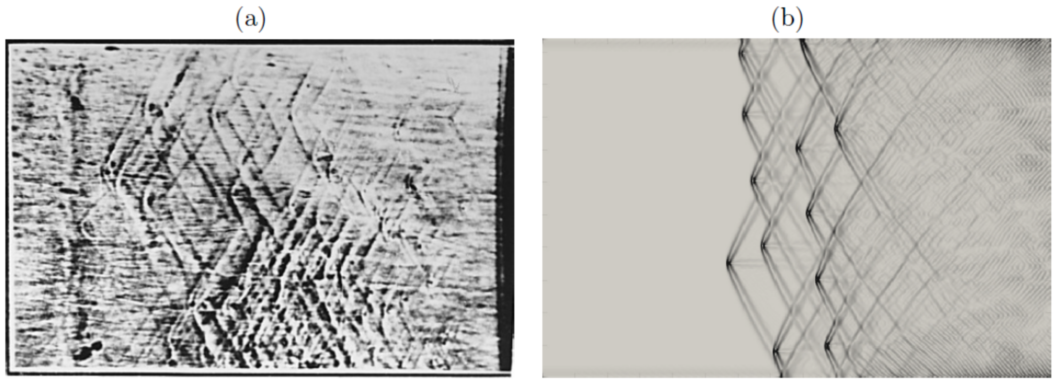

Figure 3: Experimental (a) and numerical (b) flow patterns for a small fraction of the disperse phase (0.1%).

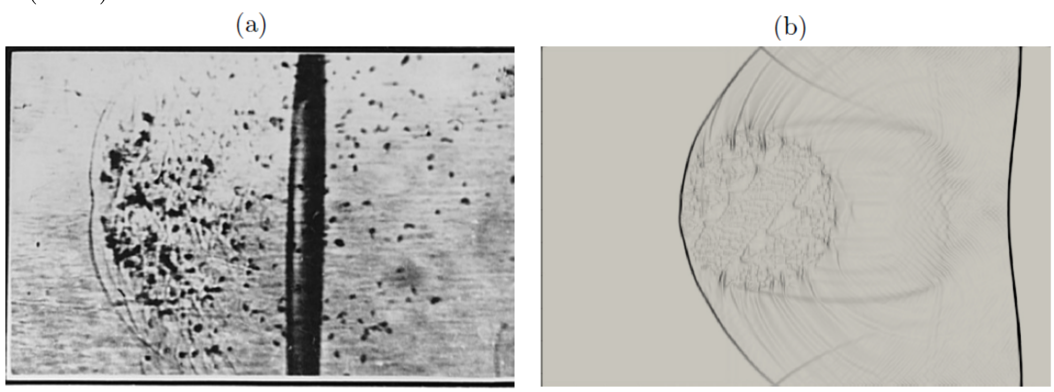

Figure 4: Experimental (a) and numerical (b) flow patterns for a large fraction of particles (1%).

The results were compared with the data obtained by optical diagnostic tools in the experiments. In both cases, we can see the formation of individual shock waves from each individual particle in the flow, as is shown in Fig. 3.

The second case considered was the behavior of the supersonic flow during its interaction with a particle cloud for a large fraction of particles. In this case, the shock waves from individual particles merge with each other and form a common shock front for the cloud, which was observed both in the experiments and numerical simulations.

At the next stage, we compared the experimental data on the dynamics of motion of the particle cloud front in the supersonic flow and the results of numerical simulations for various models of the drag force calculation.

For the particle fraction of 0.1%, good agreement is observed for model 2 and model 3, while the classical model where supersonic effects are ignored yields significant differences. For the particle fraction of 1%, there is still good agreement with experimental data, and the difference between the results predicted by the models decrease. Presumably, this can be caused by the fact that the supersonic flow passing through a dense cloud of particles becomes more decelerated, and the flow approaches the subsonic velocity, as is seen in Fig. 6.

Similar results were also obtained for the second set of experiments with plastic particles (Fig. 7).

Thus, models 2 and 3 of gas-particle interaction yield similar results, and there are only minor differences within the experimental error. For large volume fractions of particles, model 2 is less computationally expensive. We studied the computer operation times needed for

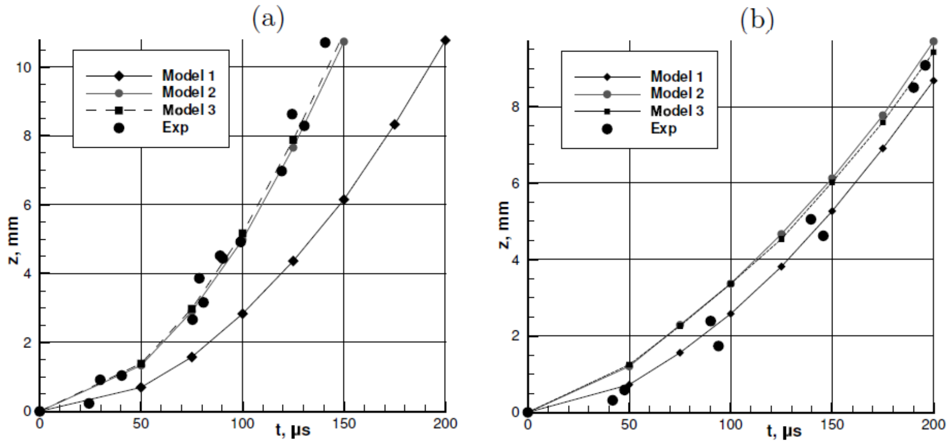

Figure 5: Dynamics of acceleration of the front of the cloud of bronze particles for the particle volume fractions of 0.1% (a) and 1% (b). Comparisons of results obtained by various models and in the experiments.

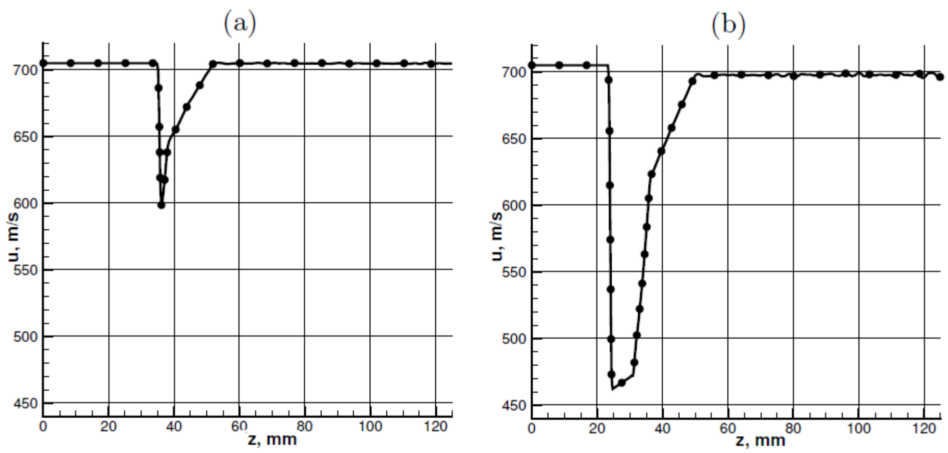

Figure 6: Gas velocity inside the particle cloud for the particle volume fractions of 0.1% (a) and 1% (b).

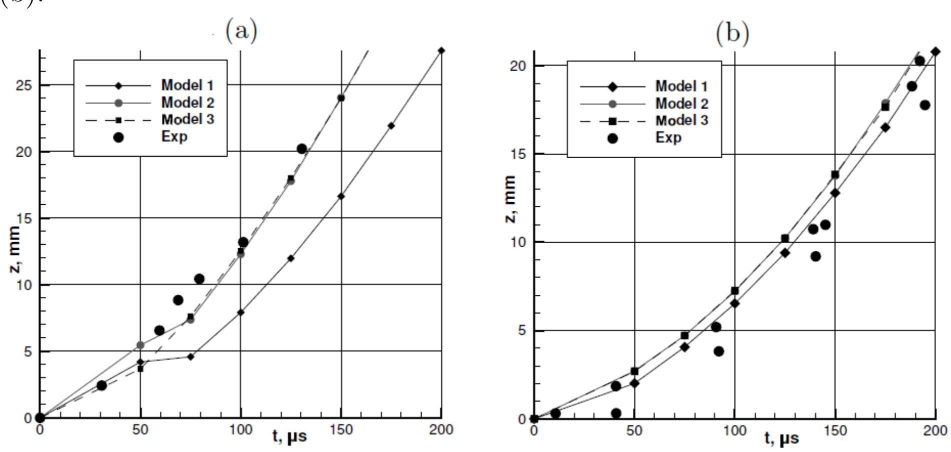

Figure 7: Dynamics of acceleration of the front of the cloud of plastic particles for the particle volume fractions of 0.1% (a) and 3% (b). Comparisons of results obtained by various models and in the experiments.

simulating the present experimental results. For problems with small volume fractions of particles, there was no difference in the computer times or this difference was several seconds. In the case of bronze particles with a volume fraction of 1%, the total number of particles in the computational domain was approximately 105. The computer time was 55 minutes 47 seconds if model 2 was used and 57 minutes 49 seconds if model 3 was used. The total difference in times was 3.7%. The total difference in the computer times in the problem with plastic particles was 3.5%; in this case, approximately 4×10^4 particles were present in the computational domain. It can be seen from the results that the computational cost of the models only weakly affects the computer time, but the contribution to the total computer time increases with the number of model particles and can turn out to be fairly significant for problems of larger scales.

Conclusions

Verification of the numerical technique of simulating a supersonic two-phase flow was performed. Qualitative and quantitative agreement of numerical and experimental data was obtained. The use of refined semi-empirical relations for calculating the drag force offers a fairly accurate description of the mechanisms of interphase interaction of a supersonic flow with the disperse phase with the volume fraction of particles up to 1%. Under the conditions of dense flows corresponding to those presented in the problem, the use of model 2 is an optimal decision.

Acknowledgement

The study was supported by the Russian Science Foundation (Grant No. 22-19-00750). Resources of the Equipment Sharing Center "Mekhanika" (Mechanics) were used.

References

[1] Prikhodko V.G., Khramov G.A., Yarygin V.N (1996). *Large-scale cryogenic vacuum facility for studying gas-dynamic processes*, Pribor. Tekhn. Eksper., 3, 162-164.

[2] Khodakov M.D., Zarvin A.E. Kalyada V.V. Korobeishchikov N.G. (2021). *Mass spectrometry of supersonic clustered flows of methane and methane-argon mixtures*, Vestnik of Novosibirsk State University, Series: Physics, 7(3), 84 - 95.

[3] Zaitsev A.V., Yarkov L.V. (2023). *Numerical simulation of the gas dynamics of nitrogen jets exhausting into a rarefied space*, Journal of Applied Mechanics and Technical Physics, 64(6), 979 - 986.

[4] Bird G.A. (1994). *Molecular gas dynamics and the direct simulation of gas flows*, N.Y.: Oxford University Press Inc.

[5] Nigmatulin R.I. (1987) *Dynamics of Multiphase Media*, Nauka.

[6] Gang R., Narayanan C., Subramaniam S. (2009). *A numerically convergent LagrangianвЂ“Eulerian simulation method for dispersed two-phase flows*, International Journal of Multiphase Flow, 35, 976-387.

[7] Bulat P.V., Ilyina T.E, Volkov K.N., Silnikov M.V., Chernyshov M.V (2017). *nteraction of a shock wave with an array of particles and effect of particles on the shock wave weakening*, Acta Astronautica, 135, 131-138.

[8] Sugiyama Y., Ando H., Shimura K., Matsuo A. (2019). *Numerical investigation of the interaction between a shock wave and a particle cloud curtain using a CFD-DEM model*, Shock Waves, 29, 499-510.

[9] Xu Peng, Shunyao Wang, Guoning Rao, et al. (2022). *Investigation of the Interaction Mechanism of Solid Particles under Shock Waves,*, Shock and Vibration, 3791156.

[10] Boiko V.M., Kiselev V.P., Kiselev S.P., Papyrin A.N., Poplavsky S.V., Fomin V.M. (1997). *Shock wave interaction with a cloud of particles*, Shock Waves, 7.5, 275-285.

[11] Henderson C.B. (1976). *Drag coefficients of spheres in continuum and rarefied flows*, AIAA Journal, 16.6, 707-708.

[12] OpenFOAM. URL: https://openfoam.org/

Polyansky Timofey Andreevich,
Khristianovich Institute of Theoretical
and Applied Mechanics SB RAS,
Institutskaya st. 4/1, 630090 Novosibirsk, Russia,
Email: polyansky@itam.nsc.ru

Zaitsev Alexandr Vasilevich,
Khristianovich Institute of Theoretical
and Applied Mechanics SB RAS,
Institutskaya st. 4/1, 630090 Novosibirsk, Russia,
Email: zaitsev@itam.nsc.ru

Received 01.08.2024 , Revised 10.01.2025, Accepted 15.01.2025, Available online 30.06.2025.